CHEMICAL ENGINEERING TRANSACTIONS

VOL. 45, 2015

A publication of
AIDIC
The Italian Association
of Chemical Engineering
www.aidic.it/cet

Guest Editors: Petar Sabev Varbanov, Jiří Jaromír Klemeš, Sharifah Rafidah Wan Alwi, Jun Yow Yong, Xia Liu
Copyright © 2015, AIDIC Servizi S.r.l.,
ISBN 978-88-95608-36-5; **ISSN** 2283-9216
DOI: 10.3303/CET1545173

A Computational Investigation of Hydrogen Production from Methane Steam Reactor

Grigorios Panagakos*[,a], Alexios-Spyridon Kyriakides[a], Simira Papadopoulou[a], Spyros Voutetakis[a]

[a]Laboratory of Process Systems Design and Implementation (LPSDI), Chemical Processes and Energy Resources Insitute (CPERI), Centre for Research and Technology Hellas (CERTH), 6th km Harilaou Thermi Road, P.O. Box 361 57001, Thermi, Thessaloniki, Hellas
gripanag@cperi.certh.gr

Integration of hybrid energy systems towards a sustainable future inherently relies on hydrogen-fueled devices like fuel cells whose relevant importance is justifiably increasing. Methane Steam Reforming (MSR) is currently the predominant choice for industrial and commercial hydrogen production. Permeation of H_2 through a highly selective membrane, serves for lower-than-conventional-reactors' temperature separation from the other components of the products of the MSR and simultaneous Water Gas Shift Reaction (WGSR), taking place on a catalyst layer. In this work we present a computational fluid dynamics and heat transfer investigation of such a tubular setup including an annular reactor, a Pd-Ru membrane and appropriate counter flows for inlet and outlet gases. This axially symmetric two dimensional steady state, multi-physics model aims at the systematic study of different operating conditions such as the reactor's temperature, and the methane's feed flow rate aiming at the mathematical optimization of mainly two objective functions: i.e. methane's conversion and hydrogen's recovery yield. It is found that methane conversion is favoured by elevated temperatures and lower inlet velocities of the reactant mixture, while the hydrogen recovery yield acquires a clear maximum on its temperature dependence around 743 K and benefits from diminished values of the reactants' insertion flow-rate.

1. Introduction

The realization of the reforming process can be performed either in a high temperature environment to promote the endothermic reactions, or in a catalytic environment in the presence of a highly selective towards hydrogen membrane through which H_2 permeates to an open channel. The second case is the one of a reactor (Figure 1) built in our laboratory at CPERI/CERTH and whose modelling was the initial drive for the work presented here. The actual reactor consists of two cylindrical domains, the outer one where the reaction takes place and the inner one where steam sweeps through. In the interface of the two cylinders a thin Pd-Ru membrane allows permeance only of H_2. In the same time the reactions are further catalysed by Ni-Pt particles dispersed on porous foam, composed of state of the art SiC which covers almost entirely the annulus area. 1D modelling of reformers like the work of Patel and Sunol (2007) with the addition of the burner that supplies the necessary heat, are frequent because of the ease of solution. However both experimental results and other simulations from Marino et al (2012) which compared 1D models against 2D ones, concluded that 1D models are insufficient in capturing accurately the physics. Kyriakides et al. (2014) have presented a state of the art 2D simulation of the same as ours experimental setup. This model assumes fixed thermodynamic properties, plug flow in porous medium, and disregards z direction diffusion. Further on, no resolution of the flow and temperature problem in the permeate zone are offered. We present a new, versatile, steady-state model, with the minor assumptions of pseudo-homogeneity, 2D axi-symmetry, validity of treating the gas mixtures as ideal gases and finally, validity of Sieverts law for describing hydrogen permeation through the membrane. The mass, momentum and energy balances of all compartments of the reactor and all species are solved fully coupled. Experimental

Please cite this article as: Panagakos G., Kyriakides A., Papadopoulou S., Voutetakis S., 2015, A computational investigation of hydrogen production from methane steam reactor, Chemical Engineering Transactions, 45, 1033-1038 DOI:10.3303/CET1545173

works of similar settings can be found in the literature. Barreiro et al. (2014) studied the effect of increasing the H_2O content in the system on the water gas shift reaction, studying a reactor with no sweep gas.

Angeli et al. (2013) have shown that other Ni-based catalysts showed extremely stable performance for long time at lower than 773 K temperatures. Bientinesi and Petarca (2011) have indicated the importance of two main factors for optimisation of the reformer: the feed flow rate and the temperature of the reactions. Following this reasoning, we have constructed a model and tested so far the influence of these two factors on the efficiency of the process. This efficiency is being calculated in terms of three expressions, defined as functions of the molecular flow rates F (moles/s) at the inlet and outlet for the corresponding species. These expressions are: the Hydrogen Recovery Yield (HRY), the total Hydrogen Yield (HY) and the methane Conversion Rate (MCR), as presented in Eq(1) to Eq(3):

$$CH_4 \text{ conversion} = \frac{\left(F_{CH_4}^{in} - F_{CH_4}^{out}\right)}{F_{CH_4}^{in}} \tag{1}$$

$$H_2 \text{ yield} = \frac{F_{H_2}^{out-total}}{F_{CH_4}^{in}} \tag{2}$$

$$H_2 \text{ recovery yield} = \frac{F_{H_2}^{out-perm}}{F_{CH_4}^{in}} \tag{3}$$

2. Modelling of steam reformer

The final layout of the model is shown in Figure 1.

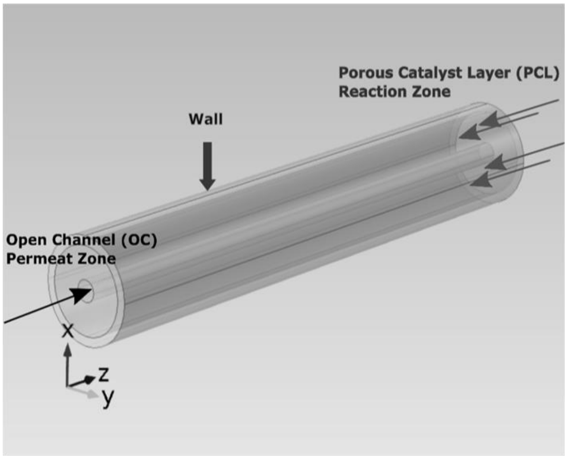

Figure 1: Computational domain

The main reactions to be taken into account are the endothermic reactions (4) and (6) and the exothermic Water Gas Shift Reaction (WGSR) (5).

$$CH_4 + H_2O \Leftrightarrow CO + 3H_2, \qquad \Delta H_{298}^0 = 206\frac{kJ}{mol} \tag{4}$$

$$CO + H_2O \Leftrightarrow CO_2 + H_2, \qquad \Delta H_{298}^0 = -41\frac{kJ}{mol} \tag{5}$$

$$CH_4 + 2H_2O \Leftrightarrow CO_2 + 4H_2, \qquad \Delta H_{298}^0 = 165\frac{kJ}{mol} \tag{6}$$

The kinetics of these reactions are incorporated in our model according to Xu and Froment (1989) through Eq(7-16). The model in r and z coordinates consists of two cylindrical domains. The outer domain is the one supporting the catalyst dispersed on the selected porous foam material. This area where the reactants CH_4 and H_2O enter and react, is from now on referred to as the Porous Catalyst Layer (PCL). The hydrogen produced along the PCL is assumed to be traversing the Pd-Ru membrane, driven from the concentration gradient and entering the Open Channel zone (OC) at which another gas in counter-flow, steam or nitrogen, sweeps it away. In both PCL and OC domains the flow is incompressible with respect to the volume of a fundamental flow element i.e. $\nabla \cdot \vec{u} = 0$, however due to the chemical reactions and H_2 permeation, the divergence of $\nabla(\rho \cdot \vec{u})$ is equal to the total mass production or depletion through the reactions and permeation.

$$R_1 = \frac{k_1}{P_{H_2}^{2.5}} \frac{\left[P_{CH_4} \cdot P_{H_2O} - \frac{P_{H_2}^3 \cdot P_{CO}}{K_1}\right]}{DEN^2}, R_2 = \frac{k_2}{P_{H_2}} \frac{\left[P_{CO} \cdot P_{H_2O} - \frac{P_{H_2} \cdot P_{CO_2}}{K_2}\right]}{DEN^2}, R_3 = \frac{3}{P_{H_2}^{3.5}} \frac{\left[P_{CH_4} \cdot P_{H_2O}^2 - \frac{P_{H_2O}^4 \cdot P_{CO_2}}{K_3}\right]}{DEN^2} \tag{7}$$

$$DEN = 1 + Ka_{H_2} P_{H_2} + Ka_{CO} P_{CO} + Ka_{CH_4} P_{CH_4} + K_{aH_2O} \frac{P_{H_2O}}{P_{H_2}} \tag{8}$$

$$k_n = A_n \exp\left(-\frac{E_{1,n}}{Rg \cdot T}\right), \quad n = 1,2,3 \tag{9}$$

$$K_n = B_n \exp\left(-\frac{E_{2,n}}{Rg \cdot T}\right), \quad n = 1,2,3 \tag{10}$$

$$Ka_l = Ba_l \exp\left(-\frac{E_{a_l}}{Rg \cdot T}\right), \quad l = CH_4, H_2O, H_2, CO \tag{11}$$

$$R_{H_2} = (3R_1 + R_2 + 4R_3) \cdot M_{H_2} \tag{12}$$

$$R_{CH_4} = -(R_1 + R_3) \cdot M_{CH_4} \tag{13}$$

$$R_{H_2O} = -(R_1 + R_2 + 2R_3) \cdot M_{H_2O} \tag{14}$$

$$R_{CO} = (R_1 - R_2) \cdot M_{CO} \tag{15}$$

$$R_{CO_2} = (R_2 + R_3) \cdot M_{CO_2} \tag{16}$$

As a result, the densities exhibit spatial gradients throughout the computational domains.
In the open channel the continuity for the mixture of steam and hydrogen takes the form:

$$\vec{u}_{oc} \cdot \nabla(\rho_{oc} \omega_m) = \nabla(\rho_{oc} D_{H_2-H_2O} \nabla \omega_m) + R_m \tag{17}$$

ω_m is the mass fraction, $D_{H_2-H_2O}$ is the binary diffusion coefficient at the current temperature, and R_m is the reaction rate, while $m = H_2O, H_2$. The Navier-Stokes equation in the same domain is written as:

$$\vec{u}_{oc} (\vec{u}_{oc} \nabla) \rho_{oc} + \rho_{oc} \vec{u}_{oc} \cdot \nabla \vec{u}_{oc} = -\nabla P_{oc} + \mu_{oc} \nabla^2 \vec{u}_{oc} \tag{18}$$

$\vec{u}_{oc}$ is the velocity, P_{oc} is the pressure and μ_{oc} is the dynamic viscosity of the gas mixture, based on the actual spatial gas composition in the open channel. In the PCL the mass conservation for the individual species results in the convection-diffusion-reaction equation:

$$\vec{u}_{pcl} \cdot \nabla(\rho_{pcl} \omega_i) = \nabla(\rho_{pcl} D_i \nabla \omega_i) + R_i \tag{19}$$

In the above expression ω_i is the mass fraction, D_i is the multi-component Stefan-Maxwell diffusion coefficient at the current temperature, and R_i is the reaction rate while $i = CH_4, H_2O, H_2, CO_2, CO$.
The momentum flow through the porous medium is described by the Brinkman equation.

$$\frac{\rho_{pcl}}{\varepsilon}\left((\vec{u}_{pcl} \cdot \nabla)\frac{\overrightarrow{u_{pcl}}}{\varepsilon}\right) = -\nabla P_{pcl} + \frac{\mu_{pcl}}{\varepsilon} \nabla^2 \vec{u}_{pcl} + \left(\boldsymbol{\kappa}^{-1} \mu_{pcl} + \frac{\Omega}{\varepsilon^2}\right)\vec{u}_{pcl} \tag{20}$$

Where, Ω is the total mass production/depletion, ρ_{pcl} is the density, P_{pcl} is the pressure, $\vec{u}_{pcl}$ is the velocity, $\boldsymbol{\kappa}$ is the permeability tensor and μ_{pcl} is the dynamic viscosity of the gas mixture, based on the actual spatial gas composition, flowing through the pores.
The membrane is modelled as a boundary condition on the interface of the two domains. The hydrogen flux in $\mathrm{mol/(m^2 s)}$ that goes through the membrane is modelled by the semi-empirical Sieverts law:

$$\vec{J}_{H2siev} = \frac{Q\cdot \exp\left(-\frac{E_a}{Rg\cdot T}\right)}{d_m}\left(P^{0.5}_{H2_{pcl}} - P^{0.5}_{H2_{oc}}\right) \tag{21}$$

Where Q is the pre-exponential factor of hydrogen permeability, E_a is the activation energy and d_m is the membrane's thickness. The overall endothermic nature of the process renders indispensable resolving the heat problem of the reformer as well. The outer wall of the PCL is considered to be maintained at a constant temperature, approximately 823 K. All other gases are supposed to be entering the reactor at 100 K lower temperatures. In the open channel the heat profile is being generated by solution of the following equation:

$$\rho\, c_{P_{oc}}\ \vec{u}_{oc}\nabla T_{oc} + \nabla\cdot\left(-k_{oc}\nabla T_{oc}\right) = 0 \tag{22}$$

The heat capacity under constant pressure is being calculated as a function of the spatial distribution of composition and temperature. The energy balance for describing the average temperature distribution in the PCL, comprising of the gas mixture and the porous medium is given by the following equation:

$$\rho_{pcl}\ c_{Ppcl}\ \vec{u}_{pcl}\nabla T_{pcl} + \nabla\cdot\left(-k_{pcl}\nabla T_{pcl}\right) = S_T \tag{23}$$

The average heat conduction and heat capacity coefficients are assumed to be the linear combination of the pore and solid phase's relevant coefficients.

$$\begin{aligned} k_{pcl} &= \varepsilon\cdot k_{pcl_{mix}} + (1-\varepsilon)k_{pcl_{foam}} \\ c_{Ppcl} &= \varepsilon\cdot c_{Ppcl_{mix}} + (1-\varepsilon)c_{Ppcl_{foam}} \end{aligned} \tag{24}$$

Once again, the gas mixture's properties are functions of composition and temperature profiles and all gases are treated as ideal. The heat source/sink term S_T originates from the reactions involved, accordingly to their thermochemical characteristics.

$$S_T = \rho_{catalyst}\sum_j\left(-\Delta Hr_j\right)R_j \tag{25}$$

The total hydrogen flux removed from the reaction zone and added to the permeation zone is $\pm\int_L \vec{J}_{H2siev}\,d\hat{n}$

$\pm\int_L \vec{J}_{H2siev}\,d\hat{n}$. The convection heat exchange between the reformer reaction area and the permeation zone is given by:

$$Q_{conv} = \begin{Bmatrix} -h\cdot(T_{pcl}-T_{oc}) \\ h\cdot(T_{pcl}-T_{oc}) \end{Bmatrix} \tag{26}$$

The minus sign corresponds to the heat leaving the reaction zone and the plus to the heat entering the open channel. The boundary conditions are straightforward from Figure 2. In all cases examined the Steam to Carbon ratio is 3. The pressure in the OC is 1 bar while in the PCL 10 bar.

3. Computational methodology and discretisation

The model is solved using the Finite Elements Method. We chose quadrilateral elements appropriate for axisymmetric problems. The discretisation of the computational domain is dense as dictated by the physics to be solved in order to achieve convergence and smoothness of the solution. We used 50 points in the permeate and 80 points in the retentate zone respectively along the r direction. In the z direction we used 980 points after performing mesh independence studies. Hence the maximum element size is of the order of 10^{-4}. The points in both r and z direction follow a geometrical sequence distribution so as to assign the majority of points on the boundaries of the domain where sharp gradients are anticipated. We focus our study on the parametric investigation of the changes in the temperature of the outer wall and the inlet velocity in the PCL. The spans of these studies are: $T_{sur}: 350\ \text{K} - 550\ \text{K}$ and $U_{pcl}^{inlet}: 4.51\cdot 10^{-4}\ \text{m/s} - 1.353\cdot 10^{-3}\ \text{m/s}$. The physics are solved in a fully coupled manner.

4. Results and discussion

4.1 PCL Velocity Inlet parametric study

In Figures 2 to 5, we exhibit some of the main findings coming from the parametric study on the inlet velocity of the PCL. It is reminded that reactants enter at $z = 0.4$ m while the sweep gas at $z = 0$ m for all figures that follow.

In Figure 2, we see the effect of raising the velocity on the mass fraction of methane along the reactor's length. Decreasing the velocity, results in methane being consumed almost at half the length of the reactor. Increasing the velocity ends up in extension of the length of the reactor needed for full conversion. This result is in good agreement with Figure 4, where it can be deduced that increasing the PCL inlet velocity diminishes the conversion rate.

Figure 3 is a graph of the reaction rate R_1 along the z-axis for three different radii, one close to the membrane (r_1), one in the middle of the domain (r_2) and one close to the wall (r_3). Interestingly, the picks exhibited are in descending order: $R^{MAX}_{1,\ r=r_3} > R^{MAX}_{1,\ r=r_1} > R^{MAX}_{1,\ r=r_2}$. The elevated near the wall temperature, justifies only partly this result, since the reaction rate is inherently linked not only to the temperature as seen in Eq. (4) through k_1 but on all the concentrations and the pressure as well with a highly non-linear dependence.

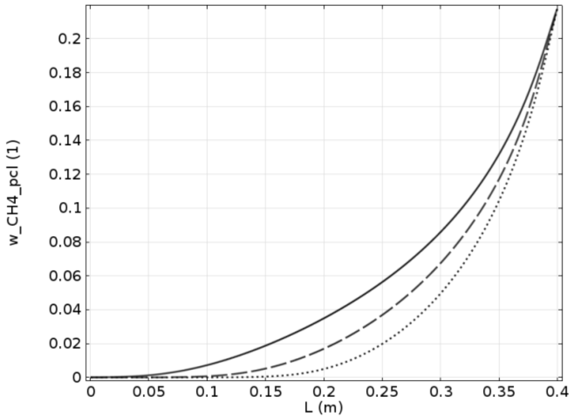

Figure 2: Methane mass fraction along a longitudinal cut in the middle of the reactor for three different pcl inlet velocities

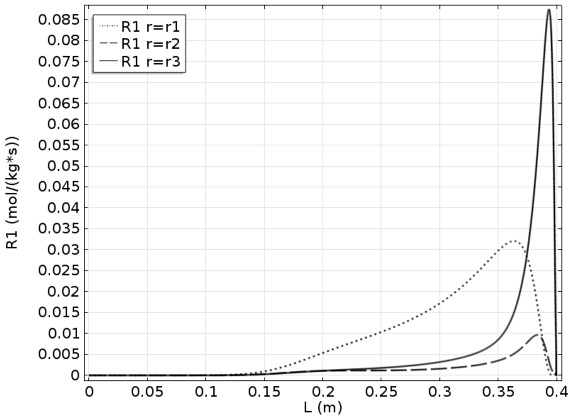

Figure 3: Hydrogen mass fraction along three longitudinal cuts. r1 close to the membrane, r2 in the middle of the reactor, r3 close to the wall

Figure 5 shows an overview of the effect of changing PCL inlet velocity on the HRY. It can be deduced that lowering the velocity increases the yield. The same trend is being observed for the total hydrogen yield.

4.2 Outer Temperature parametric study

Figures 6 and 7 sum up some of the most significant findings regarding the second parametric study. Methane conversion is favoured by elevated temperatures as anticipated and shown in Figure 6.

The counter acting forces of the reverse water gas shift reaction Eq(5) and the reforming reactions Eq(4) and Eq(6), produce a maximum for the HRY at 743 K (Figure 7).

5. Conclusions

We have produced a full 3D coupled model of a steam reformer reactor incorporating all the necessary physics with minor simplifying assumptions. The results exhibit that the methane conversion is favoured by elevated temperatures and lower inlet velocities of the reactant mixture. On the other hand, the hydrogen recovery yield has a clear maximum on its temperature dependence around 743 K while it is promoted for diminished values of reactants' insertion flow-rate.

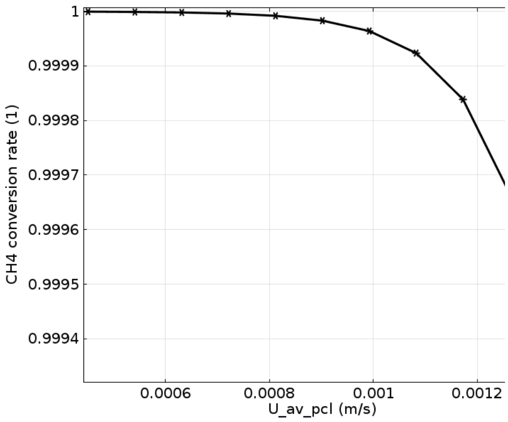

Figure 4: MCR for different PCL inlet velocities

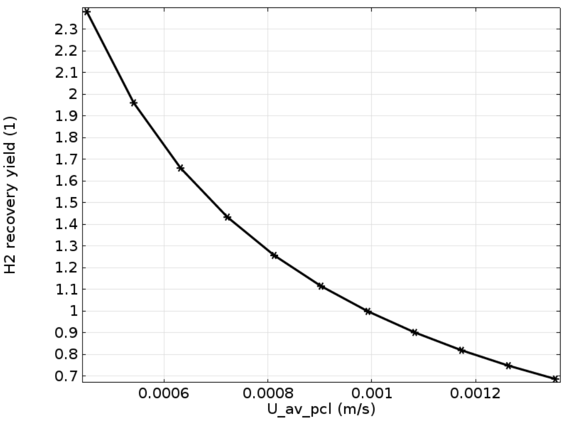

Figure 5: HRY for different PCL inlet velocities

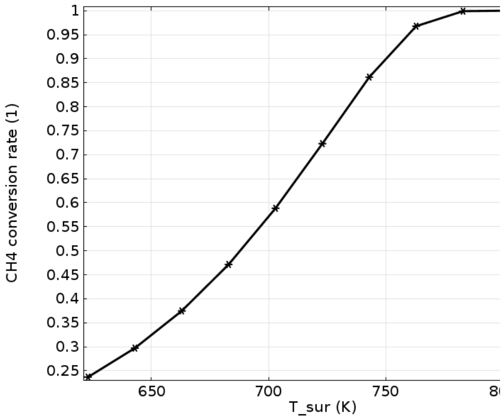

Figure 6: Methane conversion rate for different T_{sur}

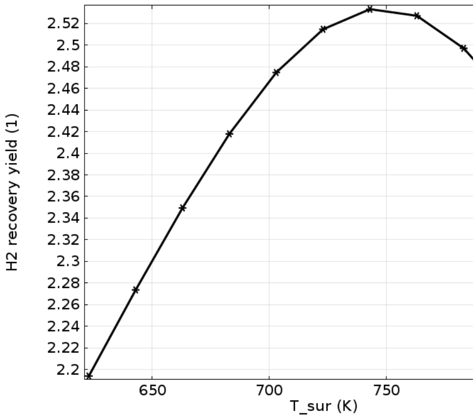

Figure 7: HRY as function of the outer wall temperature

References

Xu J., Froment G.F., 1989, Methane Steam Reforming, Methanation and Water-Gas Shift: I. Intrinsic Kinetics, AIChE Journal, 35, (1), 88-96.

Kyriakides A., Rodriguez-Garcia L., Voutetakis S., Ipsakis D., Seferlis P., Papadopoulou S., 2014, Enhancement of pure hydrogen production through the use of membrane reactor, International Journal of Hydrogen Energy, 39, 4749-4760.

Barreirio M.M, Marono M., Sanchez J.M., 2014, Hydrogen permeation through a Pd-based membrane and RWGS conversion in H_2OCO_2, $H_2/N_2/CO_2$ and $H_2/H_2O/CO_2$ mixtures. International Journal of Hydrogen Energy, 39, 4710-4716.

Patel K.S., Sunol A.K., 2007, Modelling and simulation of methane steam reforming in a thermally coupled membrane reactor, International Journal of Hydrogen Energy, 32, 2344- 2358.

Marin P., Patino Y.V., Diez F., Ordonez S., 2012, Modelling of hydrogen perm-selective membrane reactors for catalytic methane steam reforming, International Journal of Hydrogen Energy, 37, 18433-18445.

Bientinesi M., Petarca L., 2011, H_2 separation from gas mixtures through palladium membranes on metallic porous support, Chemical Engineering Transactions, 24, 763-768.

Angeli S.D., Monteleone G., Giaconia A., Lemonidou A., 2013, Low temperature methane steam reforming: Catalytic activity and coke deposition study, Chemical Engineering Transactions, 35, 1201-1206.